PCP
PLANT & CELL PHYSIOLOGY

Regular Paper

The DEAD-Box RNA Helicase AtRH7/PRH75 Participates in Pre-rRNA Processing, Plant Development and Cold Tolerance in Arabidopsis

Chun-Kai Huang[1,3], Yu-Lien Shen[1,3], Li-Fen Huang[2], Shaw-Jye Wu[1], Chin-Hui Yeh[1] and Chung-An Lu[1,*]

[1]Department of Life Sciences, National Central University, Jhongli City, Taoyuan County 320, Taiwan, ROC
[2]Graduate School of Biotechnology and Bioengineering, Yuan Ze University, Jhongli City, Taoyuan County 320, Taiwan, ROC
[3]These authors contributed equally to this work.
*Corresponding author: E-mail, chungan@cc.ncu.edu.tw; Fax, +886-3-4228482.
(Received May 21, 2015; Accepted November 18, 2015)

DEAD-box RNA helicases belong to an RNA helicase family that plays specific roles in various RNA metabolism processes, including ribosome biogenesis, mRNA splicing, RNA export, mRNA translation and RNA decay. This study investigated a DEAD-box RNA helicase, AtRH7/PRH75, in Arabidopsis. Expression of *AtRH7/PRH75* was ubiquitous; however, the levels of mRNA accumulation were increased in cell division regions and were induced by cold stress. The phenotypes of two allelic *AtRH7/PRH75*-knockout mutants, *atrh7-2* and *atrh7-3*, resembled auxin-related developmental defects that were exhibited in several ribosomal protein mutants, and were more severe under cold stress. Northern blot and circular reverse transcription–PCR (RT–PCR) analyses indicated that unprocessed 18S pre-rRNAs accumulated in the *atrh7* mutants. The *atrh7* mutants were hyposensitive to the antibiotic streptomycin, which targets ribosomal small subunits, suggesting that AtRH7 was also involved in ribosome assembly. In addition, the *atrh7-2* and *atrh7-3* mutants displayed cold hypersensitivity and decreased expression of *CBF1*, *CBF2* and *CBF3*, which might be responsible for the cold intolerance. The present study indicated that AtRH7 participates in rRNA biogenesis and is also involved in plant development and cold tolerance in Arabidopsis.

Keywords: Arabidopsis • AtRH7 • Cold stress • DEAD-box RNA helicase • Embryo development • rRNA biogenesis.

Abbreviations: AtRH, Arabidopsis RNA helicase; CBF, C-repeat binding factor; ETS, external transcribed sequence; GUS, β-glucuronidase; ITS, internal transcribed sequence; 1/2 MS, half-strength Murashsige and Skoog; MV, methyl viologen; NTC, nascent transcript cleavage; qRT-PCR, quantitative real-time polymerase chain reaction(PCR); RPL, ribosomal proteins of the large subunit; RTC, released transcript cleavage; RT–PCR, reverse transcription–PCR; WT, wild type.

Introduction

RNA helicases are enzymes that can rearrange ribonucleoprotein complexes and modify RNA structures, and are therefore involved in all aspects of RNA metabolism (Linder 2006, Hubstenberger et al. 2013, Russell et al. 2013). On the basis of the amino acid sequences and the structural features of these proteins, RNA helicases have been grouped into helicase superfamily 1 and 2 (Fairman-Williams et al. 2010). The DEAD-box family is the largest RNA helicase family and contains nine conserved motifs that constitute the helicase core domain. DEAD-box RNA helicase family members exhibit variable protein sizes and compositions of their N- and C-terminal extension sequences. These extension sequences have been proposed to provide substrate binding specificity, signals for subcellular localization or interaction domains with accessory compartments (Cordin et al. 2006, Fairman-Williams et al. 2010, Byrd and Raney 2012). Therefore, each DEAD-box RNA helicase plays a specific and crucial role in particular RNA metabolic processes, including transcription, tRNA and rRNA processing, microRNA expression and processing, mRNA splicing, RNA nucleocytoplsmic transportation, mRNA translation and RNA degradation (Rocak and Linder 2004, Cordin et al. 2006, Linder and Fuller-Pace 2013).

In total, 58 DEAD-box RNA helicases have been annotated in the Arabidopsis genome (Okanami et al. 1998, Aubourg et al. 1999, Boudet et al. 2001, Mingam et al. 2004). Certain RNA helicases have been associated with a variety of cellular functions, plant development regulation and response to abiotic and biotic stresses (Okanami et al. 1998, Aubourg et al. 1999, Boudet et al. 2001, Mingam et al. 2004). For example, AtRH3, AtRH22/HS3 and AtRH39 encode the chloroplastic DEAD-box RNA helicases involved in intron splicing and rRNA maturation in the chloroplast. Loss of function of AtRH3, AtRH22/HS3 or AtRH39 leads to abnormal chloroplast development, which is represented by a pale-green seedling phenotype (Gong et al. 2005, Kant et al. 2007, T.S. Huang et al. 2010, Xu et al. 2011, Hsu et al. 2014, Khan et al. 2014). AtRH47/ISE1, localized to mitochondria, is essential for regulation of cell–cell transport via plasmodesmata, and affects embryo development (Stonebloom et al. 2009, Burch-Smith et al. 2011). AtRH36/SWA3 is required for female gametophyte development and plays an essential role in rRNA biogenesis (C.K. Huang et al. 2010a, C.K. Huang et al. 2010b, Liu et al. 2010). AtRH57 is involved in rRNA biogenesis, glucose- and ABA-dependent

Plant Cell Physiol. 57(1): 174–191 (2016) doi:10.1093/pcp/pcv188, Advance Access publication on 3 December 2015, available online at www.pcp.oxfordjournals.org

inhibition of germination and early seedling development (Hsu et al. 2014). Three DEAD-box RNA helicases, AtRH5, AtRH9 and AtRH25, respond to multiple abiotic stresses (Kant et al. 2007, Kim et al. 2008). AtRH38/LOS4 plays a crucial role in the export of RNA molecules from the nucleus to the cytoplasm (Gong et al. 2002, Gong et al. 2005). Despite the cellular and biological functions of these RNA helicases in the various processes of RNA metabolism, development and stress responses, the functions of most DEAD-box RNA helicases in Arabidopsis remain unclear and thus require further study.

In eukaryotic cells, the 45S/35S rRNA precursor, which comprises 5′-ETS–18S rRNA–ITS1–5.8S rRNA–ITS2–25S rRNA–3′-ETS (ETS, external transcribed sequence; ITS, internal transcribed sequence), is transcribed in the nucleolus by RNA polymerase I, whereas 5S rRNA is transcribed by RNA polymerase III. The 18S, 5.8S and 25S rRNAs are formed by cleavage of the 45S/35S rRNA precursor. DEAD-box RNA helicases have been reported to play vital roles in rRNA biogenesis in several organisms (Rodriguez-Galan et al. 2013, Thomson et al. 2013, Woolford and Baserga, 2013, Ebersberger et al. 2014). In yeast and humans, 18 and 25 distinct DEAD-box RNA helicases, respectively, are required for rRNA biogenesis (Martin et al. 2013, Rodriguez-Galan et al. 2013). These DEAD-box RNA helicases are required to anneal and unwind small nucleolar RNA (snoRNA)–pre-rRNA base pairings to modulate specific chemical modifications following specific nuclease attacks, and rearrange rRNA–protein or protein–protein interactions for highly dynamic compositional changes in each rRNA processing step (Martin et al. 2013). Few RNA helicases involved in plant ribosome biogenesis have been characterized. Defects in AtRH36, AtRH57 or MTR4 result in pre-rRNA accumulation (C.K. Huang et al. 2010b, Lange et al. 2011, Hsu et al. 2014). Each of these proteins might play crucial roles at various steps of rRNA maturation, and distinct phenotypes are displayed in their knockout mutants: absence of a homozygous mutant in *atrh36* (C.K. Huang et al. 2010b); hypersensitivity to glucose inhibition of seedling growth in *atrh57* (Hsu et al. 2014); and pointed first true leaf at the first true-leaf stage in *mtr4* (Lange et al. 2011). Thus, these RNA helicases require investigation at the molecular level to determine their involvement in specific rRNA processing steps.

The At5g62190 gene encodes AtRH7/PRH75, which is a 671 amino acid protein and exhibits three conserved domains, namely DExDc, HELICc and GUCT, of the DEAD-box RNA helicases. Previous studies have demonstrated that AtRH7/PRH75 loses its helicase activity through isoaspartyl formation, which can be recovered using protein isoaspartyl methyltransferase (Nayak et al. 2013). Seeds of *atrh7/prh75* are deformed and shrunken, which indicates that AtRH7/PRH75 is crucial for seed development (Nayak et al. 2013). Although AtRH7/PRH75 targets the nucleolus (Lorkovic et al. 1997) and is presumably involved in ribosome maturation, the exact cellular function of this protein remains unknown.

This study investigated whether AtRH7/PRH75 plays a vital role in pre-rRNA processing. The results indicated that *AtRH7* expression was ubiquitous and activated in regions of cell division of plants. The expression of *AtRH7* was also induced by cold stress. Two allelic *atrh7* mutant lines displayed phenotypes that resembled the auxin-related developmental defects exhibited in several ribosomal protein mutants, and cold intolerance. Moreover, these *atrh7* mutants exhibited 18S rRNA precursor accumulation, which resulted in the delay of rRNA processing. Cold stress enhanced accumulation of the precursor. These findings indicate that AtRH7 participates in rRNA biogenesis and acts sequentially in adaptation to cold stress in Arabidopsis.

Results

AtRH7 expression is ubiquitous and active in regions undergoing cell division

Amino acid sequence analysis indicated that AtRH7 contained conserved domains of the DEAD-box RNA helicase; an N-terminal KDES domain rich in lysine (K), glutamic acid (D), aspartic acid (E) and serine (S); and a C-terminal GYR domain containing 21 glycine residues (**Supplementary Fig. S1**). An amino acid sequence-based phylogenetic analysis indicated that RH7 proteins were conserved in land plants (**Supplementary Fig. S2**) and were slightly related to human DDX21/Gu α RNA helicase.

To determine the relative expression levels of *AtRH7* in Arabidopsis, total RNAs were isolated from a variety of vegetative and reproductive tissues and were subjected to quantitative real-time PCR (qRT-PCR) with specific primers (**Supplementary Table S2**). The *AtRH7* transcript was detected in all of the selected tissues and organs, including imbibed seeds, roots, whole seedlings, stems, shoot apices, flower buds, pollens, siliques, and rosette, cauline and senescent leaves (**Fig. 1A**). To analyze the temporal and spatial expression patterns of *AtRH7*, transgenic plants expressing an *AtRH7* promoter-driven *GUS* (β-glucuronidase) chimeric gene were generated (**Fig. 1B–M**). Over 20 independent transgenic plants were obtained and three transgenic lines were selected for GUS activity analysis. GUS activity was detectable in the germinating seeds (**Fig. 1B**) as well as the seedling cotyledons and roots (**Fig. 1C**), and this activity was predominantly observed in the vegetative apex (**Fig. 1D**), veins and distal zone of the cotyledon (**Fig. 1E**), root–hypocotyl transition zone (**Fig. 1C**), root vasculature, primary root meristem and lateral root primordium of the seedling (**Fig. 1F**). GUS activity in the mature rosette leaf was primarily detected in the serrated margin and trichomes (**Fig. 1G–I**). GUS activity in the flower was primarily associated with the anthers, stigma, sepals, petals and receptacle (**Fig. 1J**). During embryogenesis, GUS activity was detected in the pre-cotyledon and root meristem at the heart (E_h) and torpedo (E_t) stages (**Fig. 1K, L**). Moreover, the cotyledon exhibited strong GUS staining, whereas the hypocotyl procambium exhibited weak GUS staining at the bent cotyledon (E_{bc}) stage (**Fig. 1M**). Thus, *AtRH7* expression was ubiquitous at all plant developmental stages examined and was detected predominantly in regions undergoing cell division.

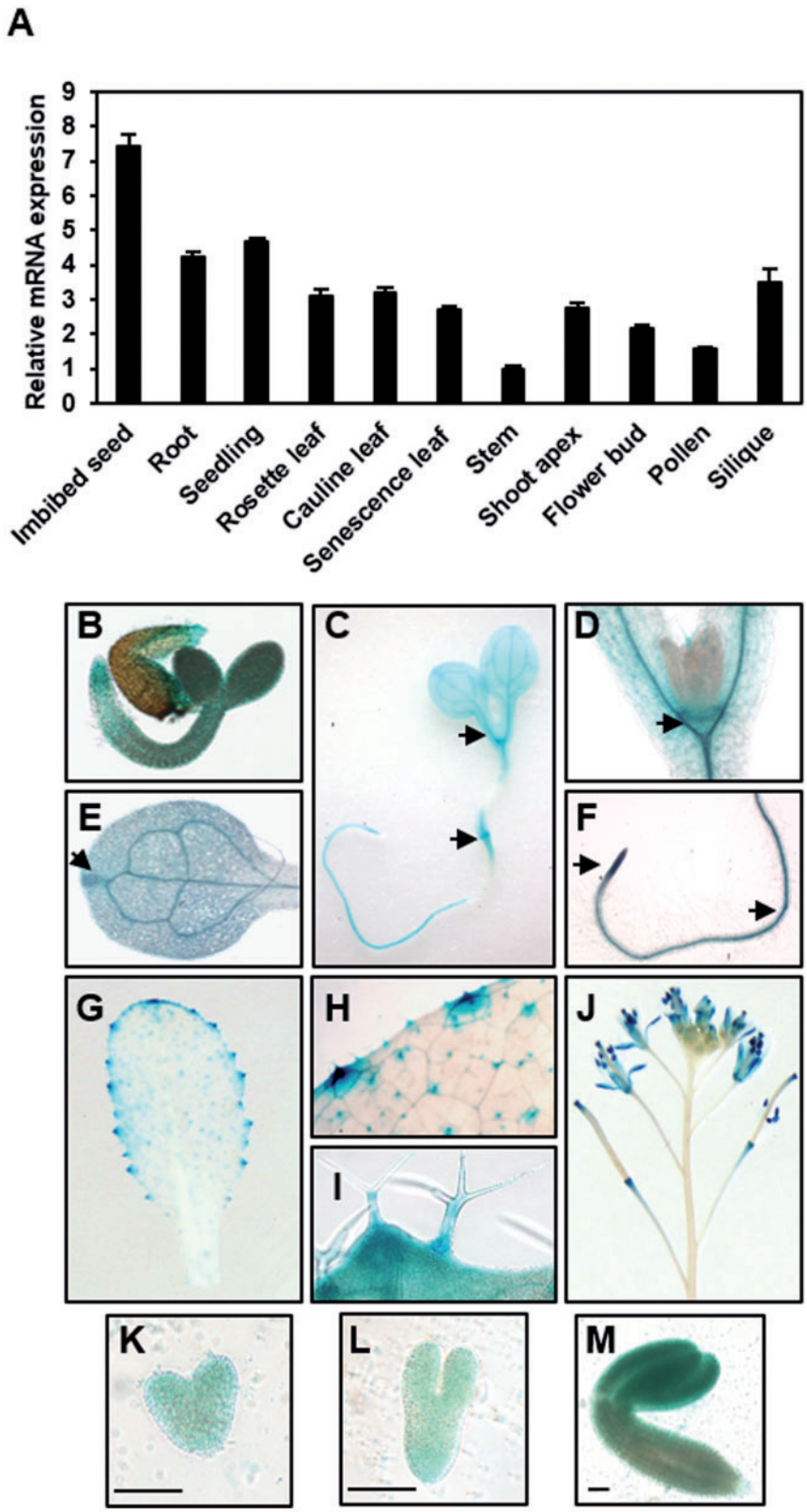

Fig. 1 *AtRH7* expression patterns. (A) Quantitative RT-PCR analysis of *AtRH7* expression in Arabidopsis. Total RNA was isolated from imbibed seeds, roots, whole seedlings, rosette leaves, stems, shoot apices, flower buds, pollens, siliques, and cauline and senescent rosette leaves. Arabidopsis *ACT1* was used as an internal control. Error bars indicate the SDs of three replicate experiments. (B–M) β-Glucuronidase (GUS) activity in *AtRH7* promoter-driven *GUS* transgenic Arabidopsis. GUS activity is shown in (B) an imbibed seed, (C) seedling, (D) seedling meristem, (E) cotyledon, (F) root, (G) rosette leaf, (H, I) leaf trichomes, (J) inflorescence, (K) heart embryo stage, (L) torpedo embryo and (M) bent cotyledon embryo. Arrows indicate areas of high GUS activity at (C) the root–hypocotyl transition zone, (D) vegetative apex, (E) distal zone of the cotyledon and (F) primary root meristem and lateral root primordium of the seedling. Scale bar = 50 μm.

AtRH7 disruption causes severe defects in plant development

To elucidate the biological and cellular functions of AtRH7, three independent T-DNA insertion mutant lines obtained from the ABRC (Arabidopsis Biological Resource Center), namely *atrh7-1* (GABI-Kat 305C08), *atrh7-2* (SALK_0606856) and *atrh7-3* (SALK_018195), were characterized and identified using genomic DNA PCR (**Supplementary Fig. S3A, B**). RT-PCR analysis detected *AtRH7* mRNAs in the *atrh7-1* mutant lines, in which a T-DNA was inserted in the *AtRH7* promoter region, but not in the *atrh7-2* and *atrh7-3* mutant lines, in which T-DNA was inserted at exon 8 and intron 7, respectively (**Supplementary Fig. S3C**). Therefore, the *atrh7-2* and *atrh7-3* mutant lines were selected to assess the role of AtRH7 in Arabidopsis. Delayed seed germination was observed in both *atrh7* mutants as compared with wild-type (WT) seeds. Seed germination rates of the *atrh7-2* and *atrh7-3* mutants were 45 ± 7.9% and 43 ± 9.5%, respectively, on day 3 (**Fig. 2A**; **Supplementary Table S3**), and >94% of seeds of both *atrh7* mutants were germinated after a 7 d incubation (**Fig. 2B**; **Supplementary Table S3**). The *atrh7-2* and *atrh7-3* seedlings displayed narrow points on the first leaves (**Fig. 2C, D**), short roots and a few branched roots (**Fig. 2E**). Some cotyledons displayed a vein structure with two closed loops, whereas dead-end veins were observed in some cotyledons of the *atrh7-2* and *atrh7-3* seedlings (**Fig. 2F**). The mature *atrh7-2* and *atrh7-3* plants exhibited a smaller overall size (**Fig. 2G, H**), as well as a 6–7 d delay in bolting (**Fig. 2G**; **Supplementary Fig S4**), compared with WT plants. After pollination, the *atrh7-2* and *atrh7-3* plants produced shorter siliques than did WT plants (**Fig. 2I, J**). The phenotypes of *atrh7-2* and *atrh7-3* mutants could be complemented fully by expression of *AtRH7* cDNA (**Supplementary Fig. S5**).

AtRH7 involvement in embryo development

The segregation ratios of the *atrh7-2* and *atrh7-3* heterozygous progeny were 1 : 2 : 0.43 (35 : 66 : 15) and 1 : 2 : 0.04 (51 : 98 : 2) (**Table 1**), respectively. The distinct reduction in the number of homozygotes among the *atrh7-2* and *atrh7-3* progeny suggests that *AtRH7* knockout may, in principle, cause defects in embryogenesis, seed germination or seedling development. However, all seeds from *atrh7-2* and *atrh7-3* heterozygotes germinated, which suggested that AtRH7 does not affect seed germination and seedling development. Therefore, embryo morphology at all stages of embryogenesis was observed and analyzed. Enlarged globular (**Fig. 3A**) and heart embryos (**Fig. 3B**) in the early stage and abnormal mature green cotyledons (**Fig. 3C**) (development of only one cotyledon, three cotyledons, or a mature green cotyledon with a twisted structure) in the late stage of embryogenesis were observed in *atrh7-2* homozygote plants. A consistent seed set was observed in the siliques of the *atrh7-3* homozygote plants (**Fig. 3A, B**). The mature *atrh7-2* mutant seeds were shrunken (**Supplementary Fig. S6**), and approximately 5% of the *atrh7-2* seedlings displayed either a single cotyledon, asymmetric cotyledons or three cotyledons (**Fig. 3D**). These results indicated that *AtRH7* deficiency caused defects in embryogenesis and initiation of asymmetric cell division.

The morphological progression of embryogenesis in Arabidopsis has been categorized into the following stages: pre-globular stage (E_{pg}), globular stage (E_g), heart stage (E_h), torpedo stage (E_t), linear cotyledon stage (E_{lc}), bent cotyledon stage (E_{bc}), mature green cotyledon stage (E_{mg}) and terminated dormant seed (**Supplementary Fig. S7A**). To examine the stage at which *AtRH7* deficiency affects Arabidopsis embryo development, *atrh7* (+/−) heterozygous mutants were observed at each stage of embryogenesis. Approximately 25% of the developing seeds exhibited abnormal morphology in the *atrh7-2* (+/−) and *atrh7-3* (+/−) heterozygotes (**Fig. 3E**); 18% and 26% pale green seeds were obtained from among 234 *atrh7-2* seeds and 258 *atrh7-3* seeds, respectively. The WT siliques exhibited synchronous seed development, with two or three sequential developmental stages (**Table 2**). However, non-synchronous seed development was observed in a silique of the *atrh7-2* (+/−) heterozygous plants; approximately 75% of the seeds were normal green and at normal developmental stages, whereas approximately 25% were pale green and their development was arrested at the globular stage with enlarged globular embryos (**Table 3**). For example, among the 40 analyzed embryos from Silique 6 (S6), four were arrested at the pre-globular stage, 12 at the globular stage, one at the torpedo stage, 20 at the linear cotyledon stage and three at the bent cotyledon stage (**Table 3**; **Supplementary Fig. S7B**). In Silique 9 (S9), 39 embryos were analyzed, of which nine were arrested at the globular stage and 30 at the mature green cotyledon stage (**Table 3**; **Supplementary Fig. S7B**). These results indicate that AtRH7 played a critical role at the globular stage during embryogenesis in Arabidopsis.

AtRH7 is necessary for tolerance to prolonged cold stress in Arabidopsis

To examine *AtRH7* expression under various stresses in Arabidopsis, 2-week-old WT seedlings were treated with cold (4°C for 12 h), osmotic (250 mM mannitol), salt (150 mM NaCl), drought (10 min air drying), heat (37°C for 3 h) or oxidative [5 μM methylviologen (MV)] stresses. Total RNAs were isolated and subjected to qRT-PCR analysis. The level of *AtRH7* transcripts was not affected in the seedlings under osmotic, salt, drought and heat stresses; however, the cold-stressed seedlings exhibited a 3-fold increase in *AtRH7* mRNA expression levels (**Fig. 4A**). These results indicated that *AtRH7* expression responds to cold stress and that AtRH7 may participate in cold tolerance. To assess their cold tolerance capability, WT, *atrh7-2* and *atrh7-3* seedlings were grown in growth chambers at 4 and 22°C, and their seedling morphologies were compared. The *atrh7-2* and *atrh7-3* seedlings grown at 4°C displayed more severe phenotypes of growth retardation, a pointed first leaf and pale green true leaves compared with the *atrh7-2* and *atrh7-3* seedlings grown at 22°C (**Fig. 4B–D**). Under prolonged cold stress, the leaves of *atrh7-2* and *atrh7-3* plants became withered and purple-colored (owing to anthocyanin accumulation) and eventually died (**Fig. 4D**), whereas the leaves of WT

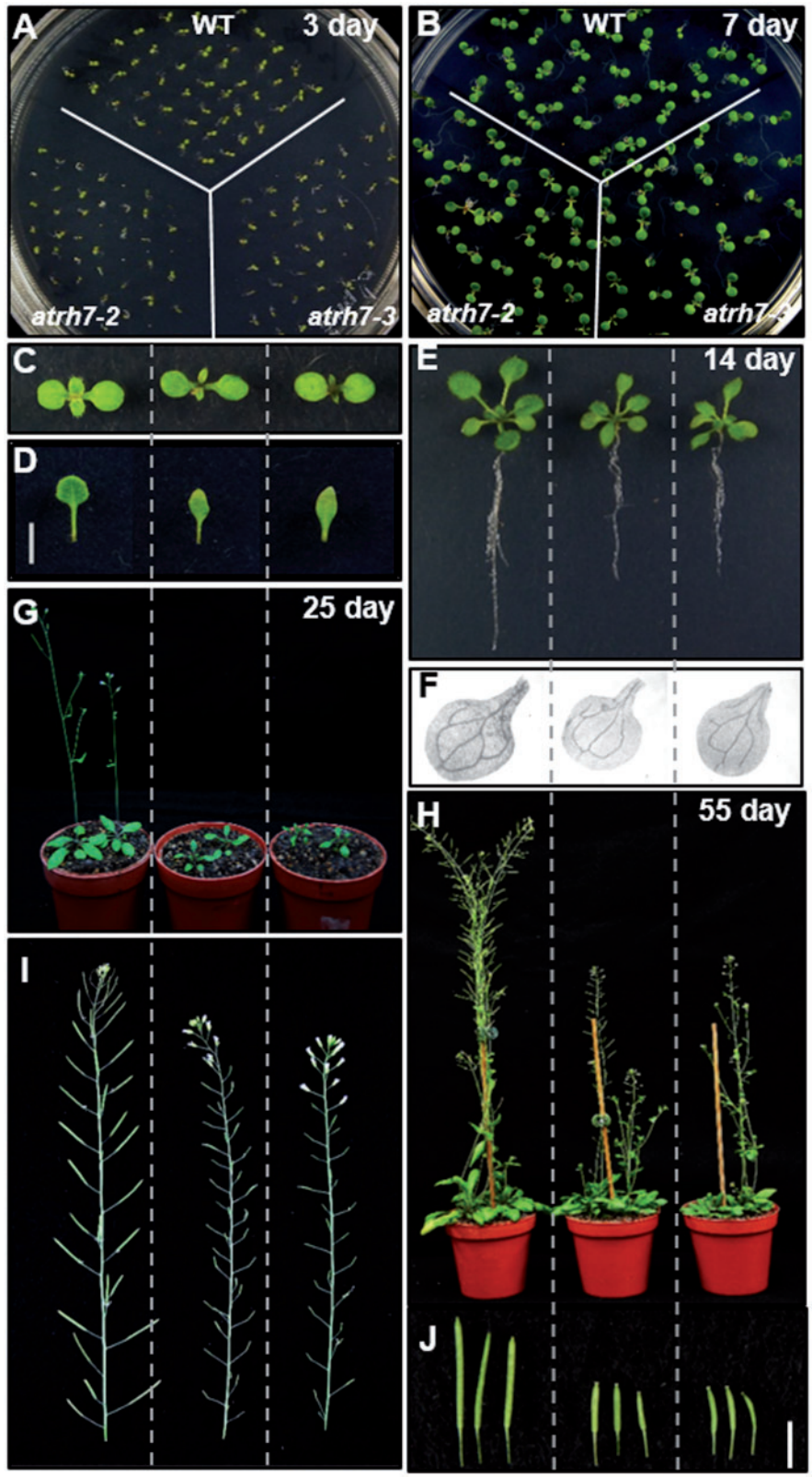

Fig. 2 Phenotypes of the Arabidopsis *atrh7* mutants. (A) Wild-type (WT), *atrh7-2* and *atrh7-3* seeds were germinated on 1/2 MS medium supplemented with 1% sucrose for 3 d. (B) WT, *atrh7-2* and *atrh7-3* seedlings were grown on 1/2 MS medium supplemented with 1% sucrose for 5 d. (C) The first true leaves of WT, *atrh7-2* and *atrh7-3* seedlings. (D) Two-week-old WT, *atrh7-2* and *atrh7-3* seedlings. (E) Cotyledon vein patterns of WT, *atrh7-2* and *atrh7-3* seedlings. (F, G) WT, *atrh7-2* and *atrh7-3* mutants were grown in pots under normal conditions for 35 d (F) and 55 d (G). (H) Inflorescence of the WT, *atrh7-2* and *atrh7-3* mutants. (I) WT, *atrh7-2* and *atrh7-3* mutant siliques. Scale bar = 1 cm.

Table 1 The progeny genotypes from self-crossed wild-type and heterozygous mutant plants

Parental genotype	No. of progeny			χ^2 test
	+/+	+/m	m/m	
WT	41	–	–	$P = 1$
atrh7-1/AtRH7	4	11	5	$P = 0.86$
atrh7-2/AtRH7	35	66	15	$P = 2.94E-3$
atrh7-3/AtRH7	51	98	2	$P = 5.53E-11$

+, wild-type allele; m, the mutant allele.

Table 2 Synchrony of embryogenesis in various developmental siliques in wild-type Arabidopsis

Silique	No. of seeds at developmental stages							Total embryos
	E_{pg}	E_g	E_h	E_t	E_{lc}	E_{bc}	E_{mg} [a]	
S1	34	8						42
S2		32	1					33
S3		20	19					39
S4		4	40					44
S5		2	12	31				45
S6				4	48			52
S7						58	10	68
S8							44	44

[a] Pre-globular stage (E_{pg}), globular stage (E_g), heart stage (E_h), torpedo stage (E_t), linear cotyledon stage (E_{lc}), bent cotyledon stage (E_{bc}) and mature green cotyledon stage (E_{mg}).

Table 3 Delayed embryogenesis in the globular stage in various developmental siliques in *atrh7* heterozygous Arabidopsis

Silique	No. of seeds at developmental stages							Total embryos
	E_{pg}	E_g	E_h	E_t	E_{lc}	E_{bc}	E_{mg} [a]	
S1		5	15					20
S2	1	9		14	10			34
S3	4	4		1	17			26
S4	3	7		16	10			36
S5	3	8		7	16	1		35
S6	4	12		1	20	3		40
S7		6				28		34
S8		4			4	8	17	33
S9		9					30	39

[a] Pre-globular stage (E_{pg}), globular stage (E_g), heart stage (E_h), torpedo stage (E_t), linear cotyledon stage (E_{lc}), bent cotyledon stage (E_{bc}) and mature green cotyledon stage (E_{mg}).

plants remained green and healthy (**Fig. 4D**). These results indicated that AtRH7 plays a positive role in cold tolerance in Arabidopsis.

To investigate the mechanism by which AtRH7 enhanced cold tolerance, 2-week-old WT, *atrh7-2* and *atrh7-3* seedlings were subjected to cold stress for 4–48 h, after which *CBF1* (*C-repeat binding factor 1*), *CBF2*, *CBF3* and *COR15a* expression patterns were examined. The level of *AtRH7* mRNA was increased by cold treatment, peaked at 24 h of cold treatment and then decreased slightly under cold stress for 48 h (**Fig. 5A**). The WT seedlings exhibited increased *CBF1*, *CBF2* and *CBF3* expression levels under cold stress for 4, 8, 12, 24 and 24 h (**Fig. 5B**). In contrast, the expression levels of *CBF* induced by cold stress were markedly lower in the *atrh7-2* and *atrh7-3* seedlings (**Fig. 5B**). In addition, the mRNA levels of a CBF downstream gene, *COR15a*, were markedly lower in the *atrh7-2* and *atrh7-3* seedlings than in WT seedlings (**Fig. 5**). These results indicate that AtRH7 is vital for the CBF-mediated cold response system in Arabidopsis.

AtRH7 participates in rRNA biogenesis

rRNA biogenesis occurs in the nucleolus with transcription of the 45S/35S rRNA precursors by RNA polymerase I and multiple processing steps of two alternative processing mechanisms: nascent transcript cleavage (NTC) and released transcript cleavage (RTC) (Lafontaine et al. 1995, Kressler et al. 1999, Hang et al. 2014). AtRH7 is localized in the nucleolus (Lorkovic et al. 1997); therefore, rRNA biogenesis processing in *atrh7-2* and *atrh7-3* plants was examined. Two-week-old WT, *atrh7-2* and *atrh7-3* seedlings were grown in a non-stress condition (22°C) and under cold stress (4°C). Total RNAs were isolated from the seedlings and subjected to qRT-PCR to evaluate the abundance of the rRNA precursor. Specific primers were designed to detect the various regions of 35S pre-rRNA (**Supplementary Fig. S8A**). In the non-stressed condition, the 5′-ETS, ITS1, ITS2 and 3′-ETS levels were about 2-fold higher in the *atrh7-2* and *atrh7-3* plants compared with the WT plants (**Supplementary Fig. S8B**). This result indicated that AtRH7 participates in 45S/35S pre-rRNA processing in Arabidopsis. The relative levels of 5′-ETS and ITS2 fragments in cold-stressed seedlings were 2.5-fold higher in the *atrh7-2* and *atrh7-3* plants than in the WT plants (**Supplementary Fig. S8B**), and the relative levels of ITS1 fragments were 4.5- and 6-fold higher in the *atrh7-2* and *atrh7-3* plants under cold stress, respectively, than in WT plants (**Supplementary Fig. S8B**).

To examine further the accumulated pre-rRNAs in the *atrh7* mutants, total RNAs were isolated from either the control or cold-stressed WT, *atrh7-2* and *atrh7-3* plants, and then subjected to Northern blot analysis with specific probes (**Fig. 6A**).

Three fragments, namely 35S/33S, 32S and P-A3/P-A2, were detected using the 5′-ETS probe (S5) (**Fig. 6B**). The accumulated levels of the 35S/33S fragment were higher in the *atrh7* mutants than in the WT mutants, regardless of whether they were treated with cold or not, whereas levels of 32S and P-A3/P-A2 were only markedly increased in *atrh7* mutants under cold treatments. Three ITS1 probes, S7, P42 and P43, were used to detect pre-rRNAs. Taking all data from ITS1 probes together, fragments of 35S/33S, 32S, 27SA(?), P-A3/P-A2 and 18S-A3/18S-A2 were detected (**Fig. 6B**). The accumulated levels of these pre-rRNAs in the *atrh7* mutants were higher than those in the WT, except for that of the P-A3/P-A2 (**Fig. 6B**). Cold stress treatments further increased the levels of 35S/33S, 32S, 27SA(?), P-A3/P-A2 and 18S-A3/18S-A2 in the *atrh7* mutants

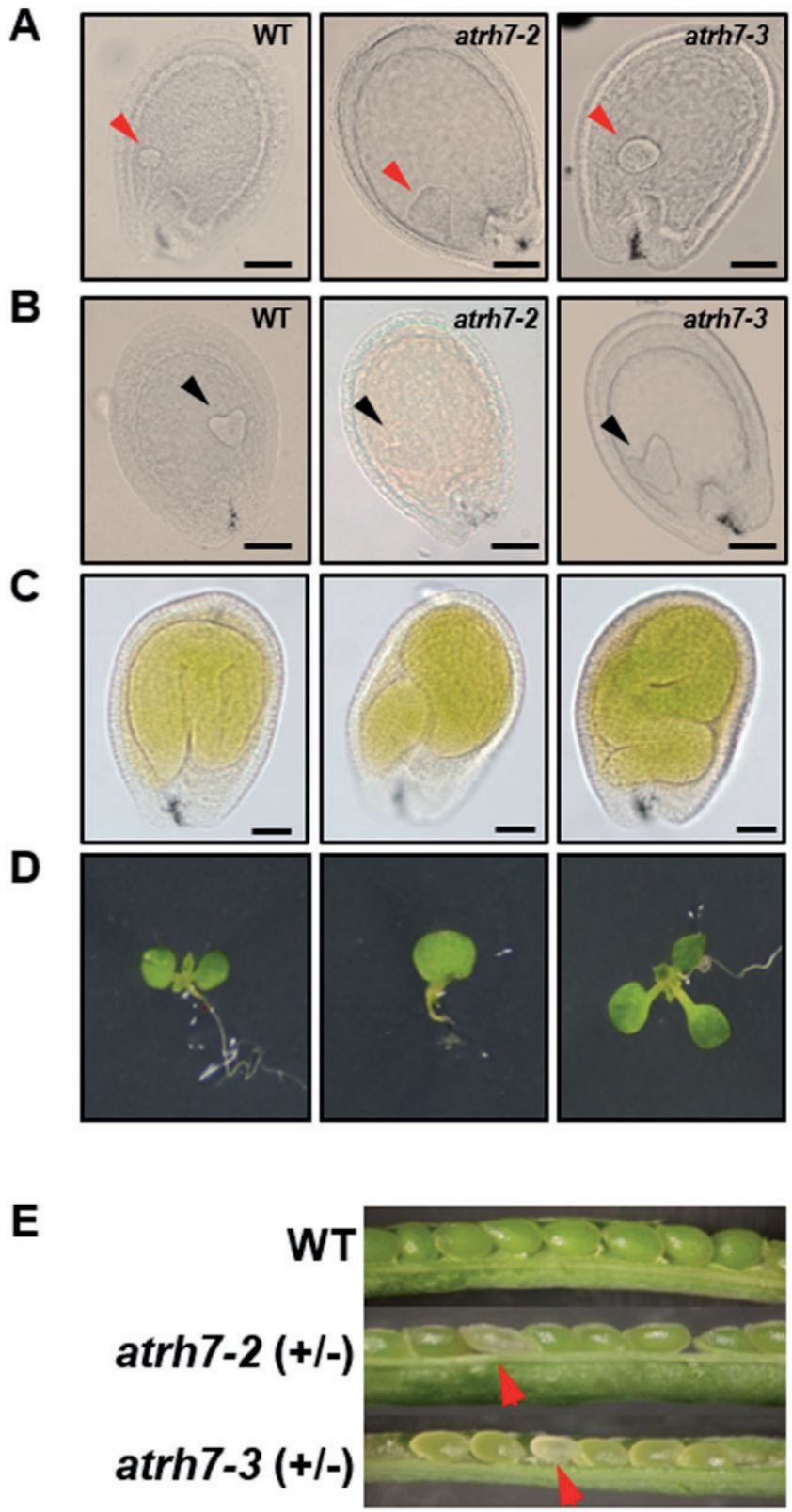

Fig. 3 Seed development in the developing siliques of *atrh7-2* homozygous and *atrh7-2* (+/−) heterozygous plants. (A) The developing siliques of the *atrh7-2* and *atrh7-3* homozygous mutants exhibited abnormal embryo development in the globular stage. The globular embryos are indicated by red arrows. (B) Developing siliques of the *atrh7-2* and *atrh7-3* homozygous mutants exhibited abnormal embryo development in the heart stage. The heart embryos are indicated by black arrows. (C) Developing siliques of the *atrh7-2* homozygous mutants exhibited abnormal embryo development in the mature green stage. (D) Abnormal seedling morphology observed in the *atrh7-2* homozygous mutants. The *atrh7-2* homozygous seedlings exhibited single or asymmetric cotyledons. (E) The number of aborted seeds in developing siliques produced by *atrh7-2* (+/−) and *atrh7-3* (+/−) heterozygotes was higher than in developing siliques of the WT. The aborted seeds are indicated by arrows. Scale bar = 100 μm.

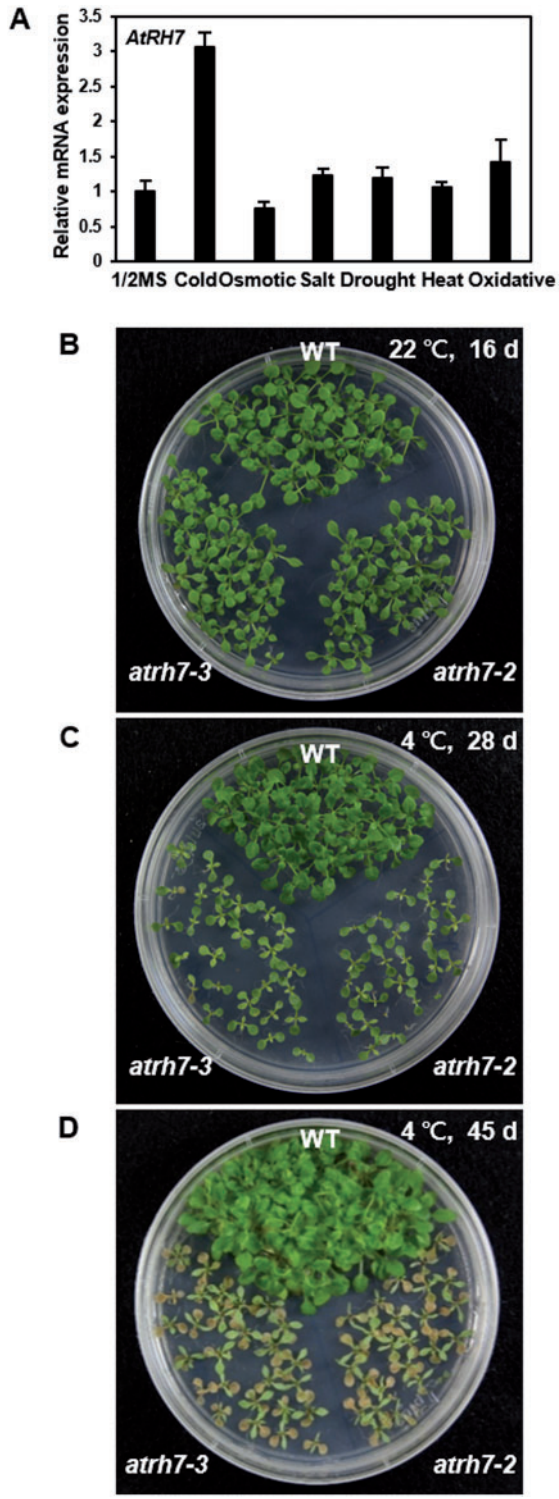

Fig. 4 Cold-intolerant phenotype in the *atrh7* mutants. (A) *AtRH7* expression patterns under various stress treatments. Two-week-old seedlings were subjected to cold (4°C for 12 h), osmotic (250 mM mannitol for 12 h), salt (150 mM NaCl for 12 h), drought (air-dried for 10 min), heat (37°C for 3 h) and oxidative (5 μM MV for 12 h) stresses. Total RNA was isolated and subjected to qRT-PCR analysis. *ACT1* was used as a control to normalize RNA signals. The qRT-PCR error bars indicate the SDs of three replicate experiments. (B–D) Comparison of the vegetative morphology of wild-type (WT), *atrh7-2* and *atrh7-3* seedlings under cold stress. The WT, *atrh7-2* and *atrh7-3* seedlings were grown at 22°C for 16 d (B), 4°C for 28 d (C) or 4°C for 45 d (D).

(**Fig. 6B**; **Supplementary Fig. S9**), and were consistent with results from qRT-PCR (**Supplementary Fig. S8B**). Using the ITS2 probe (S9) to detect pre-rRNAs, the levels of 35S/33S, 32S 27SA(?)/B and 7S pre-rRNAs were increased in the *atrh7* mutants, compared with the WT in both normal and cold stress conditions (**Fig. 6B**). The 18S (P4) and 25S (P10) probes were used as internal controls.

Circular reverse transcription–PCR (RT–PCR) was performed to determine the precise processing sites of accumulated pre-rRNAs in the *atrh7* mutants. Total RNAs of the WT, *atrh7-2* and *atrh7-3* plants were circularized by an RNA ligase and then subjected to cDNA synthesis with a specific primer, 18S cRT. Subsequently, the pre-rRNAs were amplified by PCR using the primers shown in **Fig. 7**, and the nucleotide sequences of the fragments were determined (**Supplementary Fig. S10**). The accumulated levels of P-A3 and 20S were slightly higher in the *atrh7* mutants than in the WT plants, whereas the mature 18S RNA levels did not markedly differ between the WT and the *atrh7* mutants (**Fig. 7A, B**). Using the ITS1F and c18SR primer pair, the P-A3, P′-A3 and 20S fragments were amplified, and the amount of 20S was increased in the *atrh7* mutants (**Fig. 7C, D**). Interestingly, the P-A2 fragment was amplified (**Fig. 7C, D**; **Supplementary Fig. S10**), implying that the unexpected pre-rRNA fragments could be detected by Northern blot (P-A3/PA2, **Fig. 6B**). The primer pair, 3′ETSF and 5′ETSR, was used to amplify the pre-rRNAs; higher levels of 33S and 32S (A1) were accumulated in the *atrh7* mutants than in the WT (**Fig. 7E, F**). Cold stress further increased the P-A3, 20S, 33S and 32S levels (**Fig. 7**). Taken together, these results indicate that *AtRH7* expression is required for processing mechanisms of the rRNA precursor in Arabidopsis.

The atrh7 mutants exhibit resistance to ribosomal antibiotics

To examine whether the *atrh7* mutants show defective ribosome assembly, streptomycin, spectinomycin, chloramphenicol and erythromycin were used to test the WT, *atrh7* mutants and *AtRH7* complemented plants. The WT and *AtRH7* complemented lines developed longer roots than the *atrh7* mutants in half-strength Murashige and Skoog (1/2 MS) medium (**Fig. 8A**). However, the *atrh7* mutants exhibited substantial resistance to streptomycin and produced longer roots and more intense green pigmentation in the cotyledons and leaves under 30 μg ml^{-1} streptomycin treatment than the WT or *AtRH7* complemented lines (**Fig. 8B**). In addition, the *atrh7* mutants exhibited mild resistance to 20 μg ml^{-1} spectinomycin and 10 μg ml^{-1} chloramphenicol, and a similar root length to the WT or *AtRH7* complemented lines was observed in both treatments (**Fig. 8C, D**). In contrast, the *atrh7* mutants exhibited higher sensitivity and shorter roots under erythromycin treatment, compared with those on 1/2 MS medium, but the same trend as those growth on 1/2 MS medium was observed (**Fig. 8E**). Image J software was used to calculate the lengths of roots from 15 seedlings grown in 1/2 MS medium with or without antibiotics. The relative root length patterns were similar when seedlings were grown on either 1/2 MS medium or

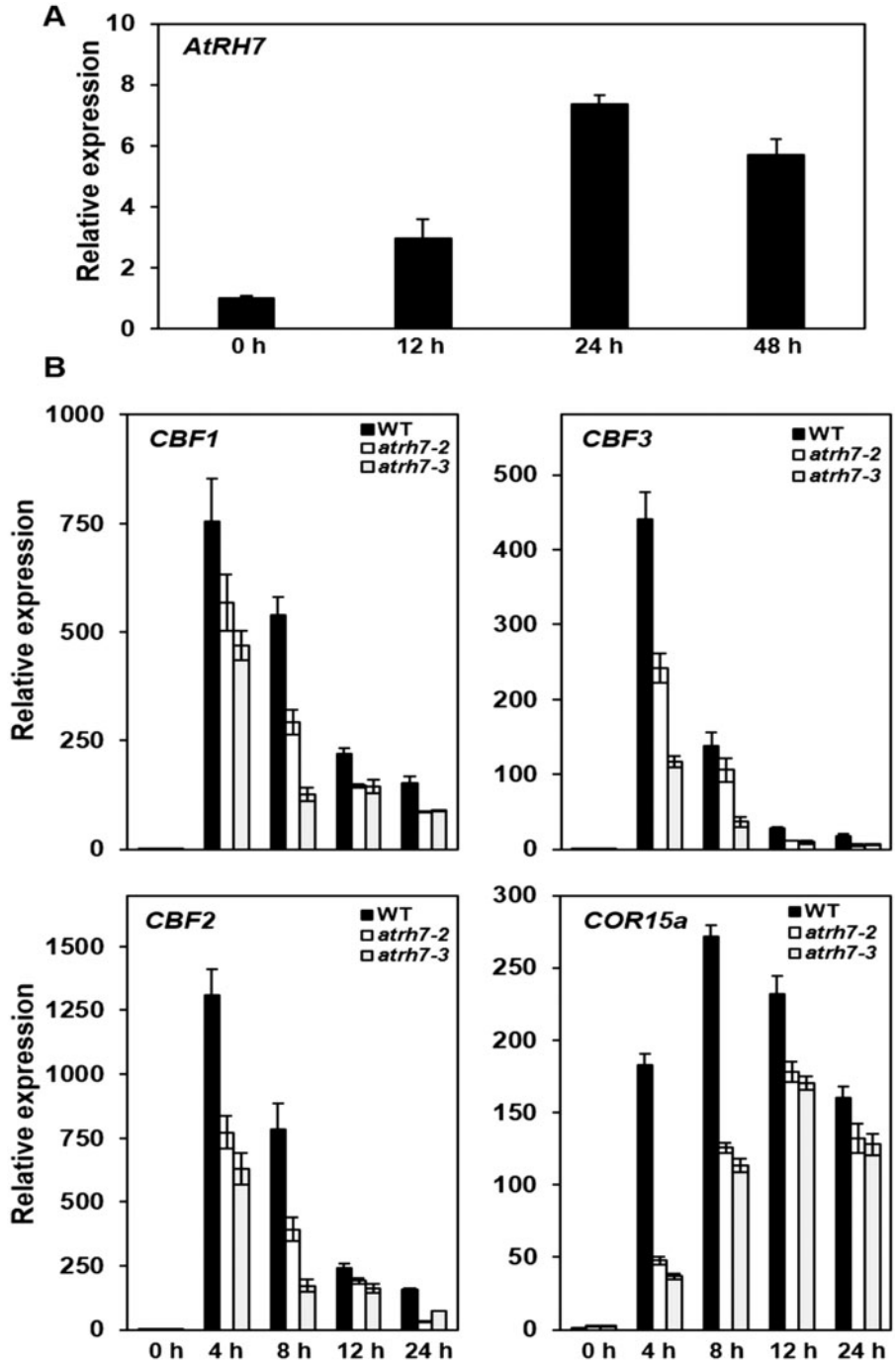

Fig. 5 Expression of cold-responsive genes in *atrh7* mutants. Total RNA was isolated from 2-week-old seedlings treated with cold stress (4°C) and then was subjected to qRT-PCR analysis. Relative mRNA expression levels were determined by normalization relative to the abundance of *ACT1* transcripts. Error bars indicate the SDs of three replicate experiments. (A) Expression of *AtRH7* in seedlings treated with cold stress for 0, 12, 24 and 48 h. (B) Expression of *CBF1*, *CBF2*, *CBF3* and *COR15a* in seedlings treated with cold stress for 0, 4, 8, 12 and 24 h.

erythromycin-containing medium, but the average root lengths of all lines on erythromycin-containing medium were shorter than those on 1/2 MS medium; whereas the *atrh7* mutants exhibited 1.5-fold longer or identical root lengths compared with those of the WT and *AtRH7* complemented lines under streptomycin, spectinomycin and chloramphenicol treatments (**Fig. 8F**). Various concentrations of antibiotics were examined, and the results showed that the *atrh7* mutants exhibited substantial resistance to streptomycin, whereas they exhibited mild resistance to spectinomycin and chloramphenicol, as compared with the WT (**Supplementary Fig. S11**). These results indicate that the *atrh7* mutation caused defects in rRNA processing and accumulation of pre-rRNA products; these effects might impact on ribosome assembly and alter ribosome conformation at antibiotic-binding sites, which would reduce specific antibiotic affinity.

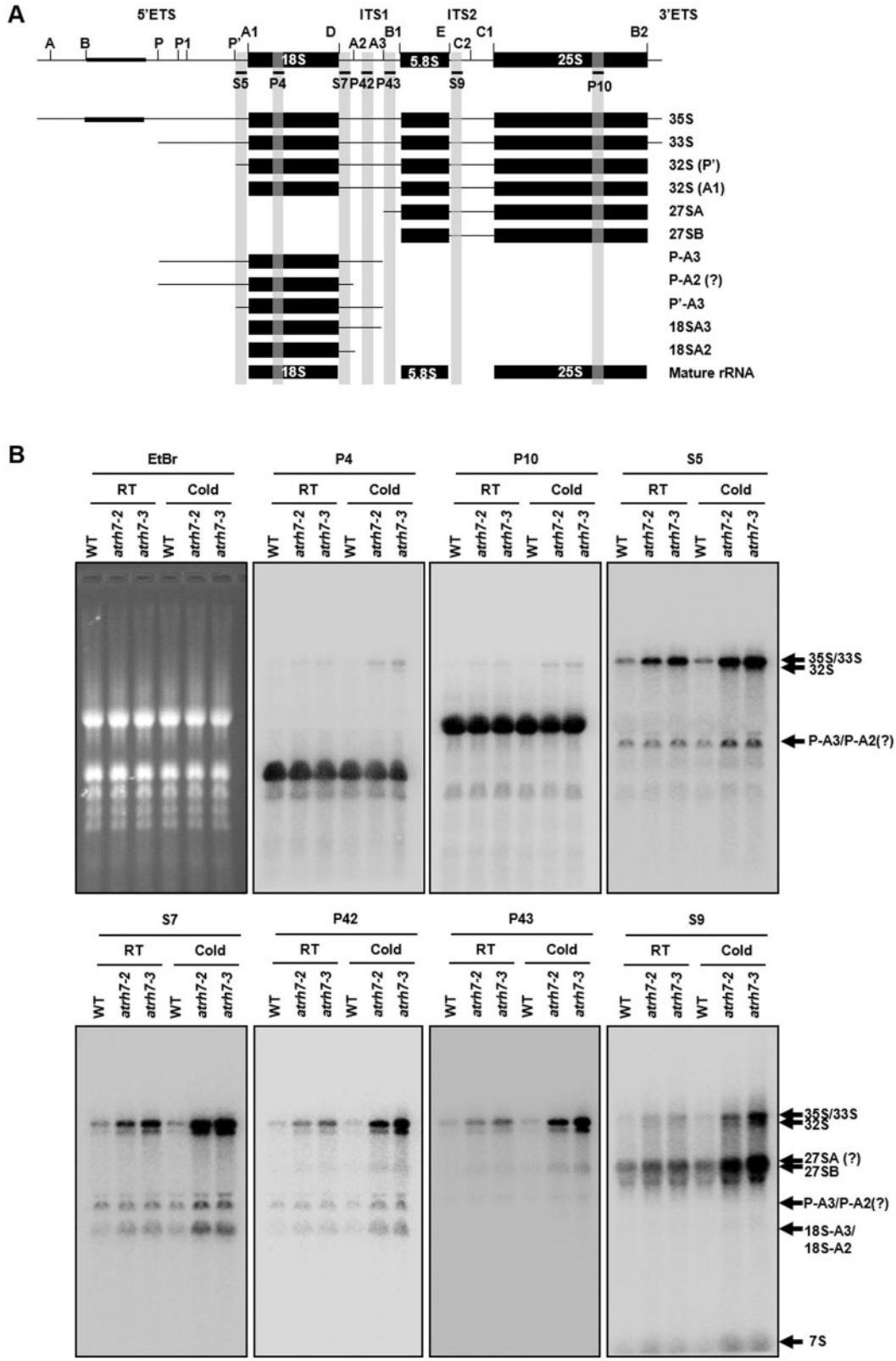

Fig. 6 Aberrant pre-rRNA processing in *atrh7* mutants. (A) Schematic illustration of the pre-rRNA structure, pre-rRNA processing sites, position of probes used for Northern blot analysis, and the expected intermediates of pre-rRNA and mature rRNA. (B) Total RNAs were isolated from 2-week-old seedlings grown at 22°C, transferred to 4°C for 7 d and then subjected to Northern blot analysis using probes specific for 18S (P4), 5′-ETS (S5), ITS1 (S7, P42 and P43), ITS2 (S9) and 25S (P10). Detected pre-rRNA and mature rRNA are indicated on the right-hand side of the diagram. EtBr staining of the gel is shown as a loading control. 18S and 25S are shown as internal controls.

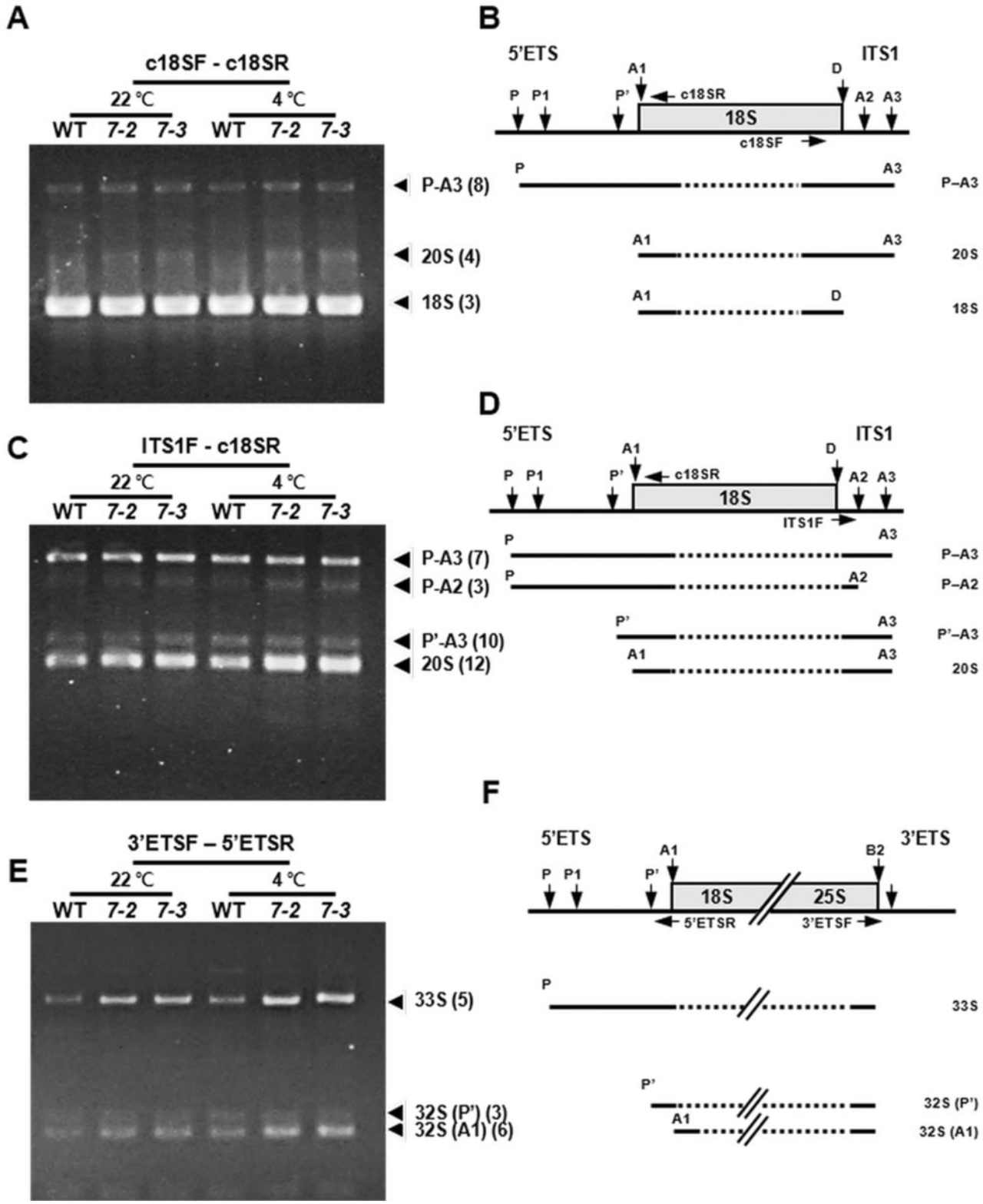

Fig. 7 Mapping of pre-RNA in *atrh7* mutants. Two-week-old seedlings of the wild type (WT), *atrh7-2* and *atrh7-3* were grown at 22 or 4°C for 7 d. Total RNA was purified, circularized and subjected to reverse transcription using 18S cRT. PCR was performed using the circularized cDNA templates and the specific primer pairs (A, B) c18SF–18SR, (C, D) ITS1F–c18SR and (E, F) 3′ETSF–5′ETSR. Mature 18S rRNA was used as an internal control. (A, C, E) The amplified fragments, indicated by arrows, were cloned and sequenced,. The number of clones of each amplified fragment is given in parentheses. (B, D, F) Illustration of the rDNA structure, primer positions for circular RT–PCR analysis and amplified fragments.

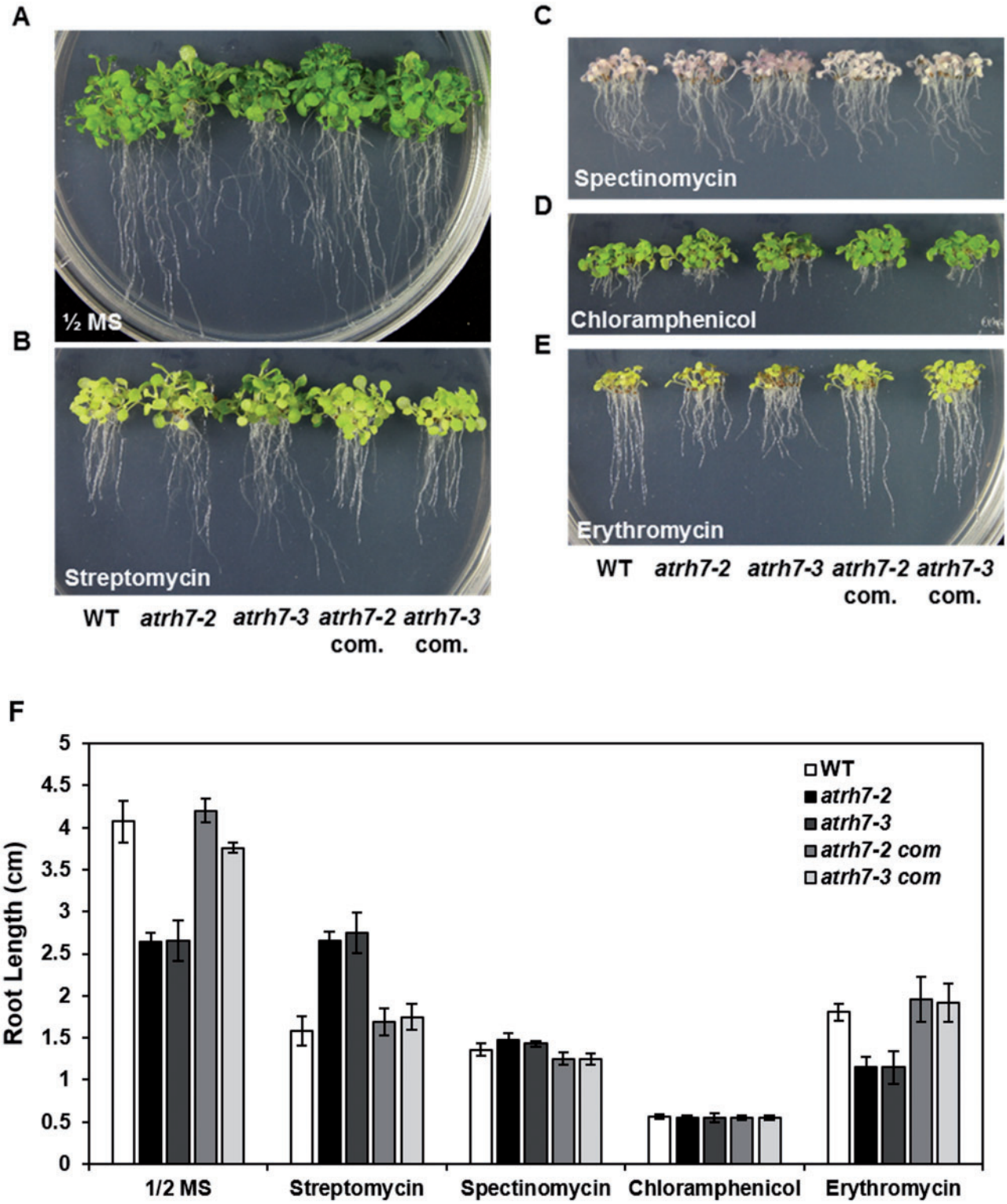

Fig. 8 Examination of the antibiotic resistance of *atrh7* mutants. The root lengths of the wild type (WT), *atrh7-2*, *atrh7-3*, *atrh7-2* complemented line and the *atrh7-3* complemented line were compared. The seeds were germinated on antibiotic-containing 1/2 MS plates and incubated vertically for root elongation analysis. The 14-day-old seedlings were grown on (A) 1/2 MS medium, or medium supplemented with (B) 30 μg ml^{-1} streptomycin, (C) 20 μg ml^{-1} spectinomycin, (D) 10 μg ml^{-1} chloramphenicol or (E) 30 μg ml^{-1} erythromycin. (F) Root lengths of seedlings grown on 1/2 MS and antibiotic-containing plates were calculated using the Image J software. Error bars indicate the SD of 15 samples.

Discussion

The *AtRH7* gene encodes a DEAD-box RNA helicase that contains double-stranded RNA-unwinding activity (Nayak et al. 2013) and localizes in the nucleolus (Lorkovic et al. 1997). The present results demonstrated that AtRH7 plays a critical role in pre-rRNA processing in both NTC and RTC mechanisms in Arabidopsis. Two allelic *atrh7* mutants, *atrh7-2* and *atrh7-3*, exhibited several developmental defects during seed germination, seedling growth and embryogenesis. In addition, the mutants displayed cold hypersensitivity and developmentally defective phenotypes of greater severity compared with the seedlings grown in the non-stressed condition. This study also provided biochemical and biological evidence for the connection between rRNA biogenesis and plant development, as well as adaptation to cold stress, in Arabidopsis.

Several reports have indicated that knockout of genes involved in rRNA biogenesis, such as *PARL1/Nucleolin*, *MTR4*, *APUM23*, *AtXRN2* and *DIM1A* (Petricka and Nelson 2007, Abbasi et al. 2010, Zakrzewska-Placzek et al. 2010, Lange et al. 2011, Wieckowski and Schiefelbein 2012, Huang et al. 2014), and those involved in ribosome assembly, such as *RPL4A*, *RPL4D*, *RPS18*, *RPL5A*, *RPL5B*, *RPL23A*, *RPL27a*, *RPL24B*/*SHORT VALVE1* (*STV1*) and *RPL28A* (Ito et al. 2000, Nishimura et al. 2005, Yao et al. 2008, Rosado and Raikhel 2010, Szakonyi and Byrne 2011), cause auxin-related phenotypes. All these mutants exhibit abnormal vein structure in cotyledons, a pointed first leaf in young seedlings, growth rate reduction in roots and short siliques in the reproductive phase. Moreover, loss of expression of *RPL24B*, *RPL4a*, *RPL4d* or *RPL5* decreases the translational levels of auxin response factors (ARFs), such as ARF2, ARF3 and ARF5, in Arabidopsis (Yao et al. 2008, Rosado et al. 2012). Auxin promotes cell growth and coincides with an increase in the total nucleic acid and protein content (Perrot-Rechenmann 2010). Recent studies have indicated that auxin action requires the modulation of ribosome biogenesis (Rosado and Raikhel 2010, Horiguchi et al. 2012). AtRH7 is involved in rRNA processing, and two allelic *atrh7* mutants display phenotypes, including abnormal vein development in the cotyledon, pointed first leaf and growth retardation in the root and shoot, similar to those of mutants of ribosomal proteins and rRNA processing factors. In addition, the expression of *AtRH7* is activated in the vegetative apex, vein, transition zone, root meristem and serrated leaf margin, which correlate with auxin-responsive cells. The present results support the hypothesis that auxin-mediated development is required to modulate ribosome biogenesis for ARF expression at the translational level of control.

The nucleolus, wherein rRNA biogenesis occurs, has regulatory functions in cell division in animal and yeast cells (Nazar 2004, Cmarko et al. 2008, Phipps et al. 2011, Woolford and Baserga 2013). The nucleolus plays a crucial role in embryogenesis in Arabidopsis (Missbach et al. 2013). For instance, a nucleolar protein, TORMOZ, is involved in 18S rRNA processing and functions in regulating the cell division plane in early embryogenesis (Griffith et al. 2007). In addition, two nucleolar proteins, AtNob1 and AtNoc4, are involved in pre-18S rRNA processing and affect the initiation of asymmetric cell division during the heart stage and, thus, enlarged globular embryos are exhibited in mutants of the respective genes (Missbach et al. 2013). The present study showed that AtRH7 plays a crucial role in pre-18S rRNA processing (**Figs. 6**, **7**) and 25% of embryos in the two allelic *atrh7* (+/−) heterozygotes showed developmental delay at the globular stage (**Table 3**). That the defect in embryogenesis caused by ribosome haploinsufficiency was observed at the globular stage suggested that cell division in the post-globular stage is regulated by the nucleolar function of 18S rRNA processing for de novo mature rRNA synthesis and ribosome assembly. However, given that *AtRH7* was asymmetrically expressed in the heart, torpedo and cotyledon stages during embryogenesis, AtRH7 might specifically participate in the regulation of cell differentiation or mitotic cell division during early embryogenesis.

Despite the fact that 25% of developing seeds exhibited abnormal development in both *atrh7* heterozygotes, a small number of *atrh7-2* and *atrh7-3* homozygotes were identified. Moreover, some of progeny can be produced from both *atrh7* homozygotes. This suggests that although AtRH7 plays a critical role during seed development, it is not essential for embryo development in Arabidopsis. In Arabidopsis, development of seeds within a given silique is usually synchronous; therefore, most seeds are matured at the same time. In the present study, asynchronous developing seeds, that might be *atrh7* homozygotes, were observed in both *atrh7* heterozygous plants. Most of the seeds with delayed development stayed at the globular stage, and few developed slowly to further stages. In turn, only very few *atrh7* homozygous seeds were produced from both *atrh7* heterozygous plants. In *atrh7* homozygotes, even development of seeds was slow but was synchronous within a given silique. The siliques of homozygotes took a longer time than those of the WT to desiccate and turn blown, and it might benefit these slowly developing homozygous seeds to have enough time to mature. Although the embryogenesis program can proceed in *atrh7* homozygous plants, defects in AtRH7 produced shrunken seeds and reduced seed number.

To adapt to cold stress, plants must control cold-stress-related gene expression. The CBF-dependent cold response pathway plays a dominant role in the development of cold tolerance in Arabidopsis (Medina et al. 2011, Zhou et al. 2011). Expression of the three *CBF* genes was reduced by 30–50% in the two allelic *atrh7* mutants compared with that in the WT plants at 4°C, probably because of weak growth and reduced rRNA biosynthesis rather than a direct impact on *CBF* gene expression at the mRNA level. However, it is also possible that AtRH7-mediated factors play roles in *CBF* gene expression to sustain cold tolerance. Thus, expression of *AtRH7* under cold stress is critical to maintain the rRNA biogenesis and essential for adaptation under low temperature in Arabidopsis.

Several DEAD-box RNA helicases have been reported to play roles in the development of cold tolerance in plants (Gong et al. 2002, Gong et al. 2005, Owttrim 2006, Vashisht and Tuteja 2006, Cartier et al. 2010, Guan et al. 2013). RCF1/AtRH42 is essential for pre-mRNA splicing and is involved in the regulation of cold-responsive gene expression to confer cold tolerance in

Arabidopsis (Guan et al. 2013). Los4/AtRH38 participates in the export of mRNAs from the nucleus to the cytoplasm and confers chilling and freezing tolerance in Arabidopsis (Gong et al. 2002, Gong et al. 2005). The involvement of RNA helicases in cold stress is also indicated in other species (Rocak et al. 2005, Cartier et al. 2010, Owttrim 2013). The most likely mechanism is that these RNA helicases serve as RNA chaperones to prevent generation of energetically stable and non-functional misfolded RNA molecules as a result of low temperature, by refolding them into the correct structure (Jarmoskaite and Russell 2011, Kuhn 2012, Guan et al. 2013, Jarmoskaite and Russell 2014). In the present study, *AtRH7* expression was induced by cold treatment. Two allelic *atrh7* mutants were cold intolerant, and pre-rRNA accumulated in the *atrh7* mutants, which further increased under cold stress. A recent study that performed a yeast two-hybrid analysis indicated that AtRH7 can interact with a cold shock domain protein, AtCSP3, which contains an RNA-binding domain and contributes to cold tolerance in Arabidopsis (Kim et al. 2013). Thus, marked activation of *AtRH7* expression is essential for the development of cold tolerance in Arabidopsis. The *AtRH7* induced by cold can either serve as an RNA chaperone or complex with AtCSP3 to maintain the pre-rRNA structure for the production of mature rRNA, thereby providing functional ribosome assembly for cold-related protein translation.

Biogenesis of rRNA is initiated with the transcription of 45S/35S pre-rRNA by RNA polymerase I in the nucleolus. Approximately 70% of the pre-rRNA is processed through NTC and the remaining 30% is processed through RTC, to generate the mature 18S, 5.8S and 25S rRNAs (Axt et al. 2014). The rRNA processing mechanism is generally conserved in eukaryotes (Sloan et al. 2013). In Arabidopsis, several pre-rRNA cleavage sites and the processing procedure differ from those in yeast and humans (Rodriguez-Galan et al. 2013, Woolford and Baserga 2013). The model of pre-rRNA processing in Arabidopsis postulates that the A2 site is cleaved/processed after removal of the 5′-ETS from P-A3 pre-rRNA (Zakrzewska-Placzek et al. 2010, Hang et al. 2014). A recent study further indicated an alternative pre-rRNA processing pathway in Arabidopsis, in which the A2 site is cleaved from 32S pre-rRNA (Weis et al. 2015). In the present study, P-A2 pre-rRNA was detected in both the WT and the *atrh7* mutants by circular RT–PCR analyses, indicating that the A2 site can be processed before 5′-ETS cleavage. Therefore, multiple ITS1 processing pathways may exist in Arabidopsis: the pre-rRNA is cleaved at the A2 or A3 site and then the 5′-ETS is removed; or the pre-rRNA is cleaved at the A3 site, then the A3 to A2 region is removed before the 5′-ETS is removed. Indeed, alternative ITS1 processing pathways have been observed in humans and yeast (Sloan et al. 2013).

A few processing factors have been proposed to be involved in specific pre-rRNA processing sites in Arabidopsis. AtXRN2 is a 5′- to 3′-dependent exonuclease that is involved in exposing the P site for cleavage (Zakrzewska-Placzek et al. 2010), and Apum23 and MTR4 are involved in the degradation of polyadenylated rRNAs (Zakrzewska-Placzek et al. 2010, Lange et al. 2011, Huang et al. 2014). The results herein indicated that AtRH7 plays a crucial role in ITS1 processing of pre-rRNA. Two allelic *atrh7* mutants accumulated a large amount of the pre-rRNA. This pre-rRNA accumulation might have been caused either by lower processing efficiency or a slower rate of pre-rRNA processing in the *atrh7* mutants than in the WT. Although the various accumulated pre-RNAs that were stalled at the A3 site cannot be distinguished in terms of whether they were derived from NTC or RTC, accumulation of 32S and 33S in the *atrh7* mutants suggested that AtRH7 functions in the A3 site processing in RTC. An alternative explanation is that accumulation of various A3 site pre-RNAs suppresses RTC processing in a similar manner to the feedback inhibition of rRNA processing hypothesized in yeast (Lafontaine et al. 1995, Kressler et al. 1999).

Ribosomes containing rRNAs and ribosomal proteins are essential for protein translation. The amount of ribosome is closely associated with cell growth and proliferation (Byrne 2009, Horiguchi et al. 2012). Several aminoglycoside antibiotics target either the small or large ribosomal subunits to inhibit translation. For instance, streptomycin binds to 16S rRNA of the bacterial ribosome, and site-specific mutation at the target site of this antibiotic results in resistance to streptomycin (Chernoff et al. 1994). Although most aminoglycoside antibiotics are weakly active against eukaryotic ribosomes, 18S rRNA has the capacity to be bound by aminoglycoside antibiotics (Kaul et al. 2005, Hobbie et al. 2007, Hua and Bedwell 2008). Moreover, mutations in eukaryotic 18S rRNA affecting translation and resistance to aminoglycoside antibiotics have been demonstrated (Kaul et al. 2005, Hobbie et al. 2007, Hua and Bedwell 2008). The *atrh7* mutants accumulated abnormal pre-18S rRNA and the seedlings were hyposensitive to streptomycin. When streptomycin bound to Arabidopsis 18S rRNA, the abnormal pre-18S rRNA assembled into the small ribosomal subunit, which then reduced the binding affinity for streptomycin. Similar results have been reported for accumulation of pre-18S rRNA in the *apum23* and *atrh57* mutants (Abbasi et al. 2010, Hsu et al. 2014), which are hyposensitive to streptomycin as seedlings.

The human RNA helicase DDX21/Gu α similar to AtRH7 interacts with ribosomal protein L4 (RPL4), which is a component of the ribosomal large subunit (Stelzl and Nierhaus 2001, Yang et al. 2005). Seedlings of the Arabidopsis *rpl4* mutant display resistance to the antibiotics chloramphenicol and erythromycin, both of which target the large subunit (Rosado et al. 2010). However, the *rpl4* mutant also exhibits hyposensitivity to streptomycin during the root growth of seedlings (Rosado et al. 2010). In *Escherichia coli*, absence of the RPL4 protein leads to elimination of the small subunit components S5, S12 and 16S rRNA (Apirion and Saltzman, 1974, O'Connor et al. 2004). Thus, although RPL4 is a component of the large subunit for protein synthesis, the absence of RPL4 can alter the whole ribosome structure, thereby reducing the binding affinity for antibiotics and resulting in resistance or hyposensitivity to antibiotics (Gabashvili et al. 2001). The *atrh7* mutants exhibited hyposensitivity to the antibiotic streptomycin, which targets the small subunit. An explanation is that abnormal pre-18S rRNA may be incorporated into the small ribosomal subunit,

which then forms aberrant ribosomes that cause hyposensitivity to streptomycin. In addition, AtRH7 may interact with RPL4; loss of *AtRH7* expression may prevent RPL4 forming the tunnel entrance site of antibiotics, as in *rpl4* mutants (Rosado et al. 2010).

Materials and Methods

Plant materials and growth conditions

All Arabidopsis (*Arabidopsis thaliana*) plants used in this study were of the Columbia (Col-0) background. The Arabidopsis T-DNA insertion mutants *atrh7-1* (GABI-Kat 305C08), *atrh7-2* (SALK_060686) and *atrh7-3* (SALK_018195) were obtained from the Salk Institute Genomic Analysis Laboratory through the ABRC. Arabidopsis seeds were surface sterilized, stratified at 4°C for 3 d in the dark, plated on 1/2 MS medium that contained 0.8% agar supplemented with 1% sucrose, and grown under a 16 h/8 h (light/dark) photoperiod (light intensity 80 μmol photons m^{-2} s^{-1}) at 22°C for 2 weeks. Two-week-old seedlings were transferred to soil and grown in the same conditions.

Primers

All primers used in this study are listed in **Supplementary Table S2**.

Plasmid construction

The *AtRH7* coding region was amplified with Hifi DNA polymerase (Yeastern) using cDNAs from 2-week-old Arabidopsis seedlings as templates and gene-specific primers (**Supplementary Table S2**), and then cloned into the T&A Cloning vector (Yeastern) to generate pAtRH7. To investigate the temporal and spatial expression patterns of AtRH7, the DNA region from 581 to 20 bp upstream of the *AtRH7* start codon was amplified by PCR using specific primers (**Supplementary Table S2**). The PCR products were digested with *Asc*I and *Pac*I and then ligated into the pMDC163 binary vector (Curtis and Grossniklaus 2003) upstream of the *GUS* gene, to generate pMDC163AtRH7GUS. For functional complementation of the *atrh7* mutants, *AtRH7* cDNA was isolated from pAtRH7 with *Asc*I and *Pac*I and then ligated into the pMDC32 vector (Curtis and Grossniklaus 2003) downstream of the *35S* promoter, to generate pMDC32AtRH7.

Quantitative RT-PCR

Total RNA was isolated using the TRIzol Reagent (Invitrogen). The RNA samples were treated with DNase and, subsequently, first-strand cDNA was synthesized from the total RNA extracted using the SuperScript III Reverse-Transcriptase kit (Invitrogen). Subsequently, a 10-fold dilution of the first-strand cDNA was subjected to qRT-PCR using FastStart Essential DNA Green Master (Roche) and an iQ5 RT-PCR machine (Bio-Rad). The procedure was independently repeated at least three times, and the relative expression of the genes was expressed as a ratio of the target gene mRNA abundance to the Arabidopsis *ACT1* (Actin-1) abundance. The data were analyzed using the iQ5 2.1 software in accordance with the manufacturer's instructions. The gene-specific primers used for qRT-PCR are listed in **Supplementary Table S2**.

Plant transformation

Agrobacterium tumefaciens strain GV3101 was used to transfer the plasmids into Arabidopsis using the floral dipping method (Clough and Bent, 1998). Transgenic plants were selected with hygromycin (25 μg ml^{-1}) and self-pollinated to generate homozygous lines.

Characterization of the *atrh7-1*, *atrh7-2* and *atrh7-3* alleles and segregation analysis

To analyze the genotypes of the progeny derived from the *atrh7-1*, *atrh7-2* and *atrh7-3* mutants, genomic DNA was isolated from 2-week-old seedlings and subjected to PCR using an LBa1 primer and *AtRH7* gene-specific primers (**Supplementary Table S2**).

AtRH7 expression analysis

Total RNA from roots, shoot apices and whole seedlings was isolated from 2-week-old seedlings grown on 1/2 MS medium. Total RNA of stems, flower buds, pollen, siliques, and rosette, cauline and senescent leaves was isolated from 6-week-old plants. In addition, total RNA was isolated from imbibed seeds stored in water for 3 d. These total RNAs were subjected to qRT-PCR to analyze *AtRH7* expression in each tissue.

Transgenic plants carrying the *AtRH7* promoter-driven *GUS* expression cassette were used for detection of GUS activity. The samples, consisting of seedlings, flowers, rosette leaves, stems and embryos, were incubated overnight in GUS staining solution at 37°C (Jefferson et al. 1987). Subsequently, Chl was extracted using 95% ethanol. The samples were observed and photographed using an Olympus IX71 inverted microscope (Olympus) equipped with a digital camera.

Embryogenesis analysis

Siliques at various developmental stages were isolated from WT and *atrh7* heterozygous and homozygous mutant plants and then incubated in Hoyer's solution (Ge et al. 1998) for 1 h. The developing seeds were observed and photographed using an Olympus IX71 inverted microscope (Olympus) equipped with a digital camera.

Northern blot analysis

Total RNA was isolated from 2-week-old seedlings treated with cold stress for 1 week, using the TRIzol Reagent (Invitrogen). A 5 μg aliquot of total RNA was separated on a 1.2% agarose gel that contained 6% formaldehyde, transferred to a Hybond N+ membrane (GE Healthcare) and hybridized at 42°C with a specific oligo DNA probe (**Supplementary Table S2**) labeled by T4 polynucleotide kinase using [γ-^{32}P]ATP. Membranes were exposed to Biomax MR film (Kodak) at −70°C.

Circular RT–PCR

For circular RT–PCR analysis (Abbasi et al. 2010), total RNA was isolated from 2-week-old seedlings grown at 22°C and from seedlings treated with cold stress (4°C) for 1 week. Following DNase treatment, the RNA samples were self-ligated using T4 RNA ligase (Invitrogen). First-strand cDNA was produced from the ligation products using the SuperScript III Reverse-Transcriptase Kit (Invitrogen) with the primers 18S cRT and 5.8S cRT. The cDNA was amplified by PCR using specific primers (**Supplementary Table S2**). The PCR products were subcloned into the T&A Cloning vector and then sequenced.

Stress treatments

To assess *AtRH7* expression in response to various abiotic stresses, 2-week-old WT seedlings grown on 1/2 MS medium were subjected to the following stress conditions for 12 h each: 4°C (cold stress); 1/2 MS medium supplemented with 250 mM mannitol (osmotic stress); 1/2 MS medium supplemented with 150 mM sodium chloride (NaCl; salt stress); or 1/2 MS medium supplemented with 5 μM MV (oxidative stress). In addition, 2-week-old WT seedlings were incubated in a growth chamber at 37°C for 3 h (heat stress) or directly air-dried for 10 min (drought stress).

Antibiotic treatments

Seeds were directly germinated on 1/2 MS medium supplemented with the following antibiotics and incubated in a growth chamber at 22°C under a 16 h/8 h (light/dark) photoperiod for up to 14 d: 30 μg ml^{-1} streptomycin (targets the small ribosomal subunit); 20 μg ml^{-1} spectinomycin (targets the large ribosomal subunit); 10 μg ml^{-1} chloramphenicol (targets the large ribosomal subunit); or 30 μg ml^{-1} erythromycin (targets the large ribosomal subunit).

Supplementary data

Supplementary data are available at PCP online.

Funding

This work was supported by the Ministry of Science and Technology of the Republic of China [grants 98-2311-B-008-002-MY3 and 103-2311-B-008-001].

Acknowledgments

We thank Dr. Su-May Yu and Ms. Sue-Ping Lee of the Institute of Molecular Biology, Academia Sinica, Taipei, for technical assistance with microscopy.

Disclosures

The authors have no conflicts of interest to declare.

References

Abbasi, N., Kim, H.B., Park, N.I., Kim, H.S., Kim, Y.K., Park, Y.I., et al. (2010) APUM23, a nucleolar Puf domain protein, is involved in pre-ribosomal RNA processing and normal growth patterning in Arabidopsis. *Plant J.* 64: 960–976.

Apirion, D. and Saltzman, L. (1974) Functional interdependence of 50S and 30S ribosomal subunits. *Mol. Gen. Genet.* 135: 11–18.

Aubourg, S., Kreis, M. and Lecharny, A. (1999) The DEAD box RNA helicase family in *Arabidopsis thaliana*. *Nucleic Acids Res.* 27: 628–636.

Axt, K., French, S.L., Beyer, A.L. and Tollervey, D. (2014) Kinetic analysis demonstrates a requirement for the Rat1 exonuclease in cotranscriptional pre-rRNA cleavage. *PLoS One* 9: e85703.

Boudet, N., Aubourg, S., Toffano-Nioche, C., Kreis, M. and Lecharny, A. (2001) Evolution of intron/exon structure of DEAD helicase family genes in *Arabidopsis*, *Caenorhabditis*, and *Drosophila*. *Genome Res.* 11: 2101–2114.

Burch-Smith, T.M., Brunkard, J.O., Choi, Y.G. and Zambryski, P.C. (2011) Organelle–nucleus cross-talk regulates plant intercellular communication via plasmodesmata. *Proc. Natl. Acad. Sci. USA* 108: 1451–1460.

Byrd, A.K. and Raney, K.D. (2012) Superfamily 2 helicases. *Front. Biosci.* 17: 2070–2088.

Byrne, M.E. (2009) A role for the ribosome in development. *Trends Plant Sci.* 14: 512–519.

Cartier, G., Lorieux, F., Allemand, F., Dreyfus, M. and Bizebard, T. (2010) Cold adaptation in DEAD-box proteins. *Biochemistry* 49: 2636–2646.

Chernoff, Y.O., Vincent, A. and Liebman, S.W. (1994) Mutations in eukaryotic 18S ribosomal RNA affect translational fidelity and resistance to aminoglycoside antibiotics. *EMBO J.* 13: 906–913.

Clough, S.J. and Bent, A.F. (1998) Floral dip: a simplified method for *Agrobacterium*-mediated transformation of *Arabidopsis thaliana*. *Plant J.* 16: 735–743.

Cmarko, D., Smigova, J., Minichova, L. and Popov, A. (2008) Nucleolus: the ribosome factory. *Histol. Histopathol.* 23: 1291–1298.

Cordin, O., Banroques, J., Tanner, N.K. and Linder, P. (2006) The DEAD-box protein family of RNA helicases. *Gene* 367: 17–37.

Curtis, M.D. and Grossniklaus, U. (2003) A gateway cloning vector set for high-throughput functional analysis of genes in planta. *Plant Physiol.* 133: 462–469.

Ebersberger, I., Simm, S., Leisegang, M.S., Schmitzberger, P., Mirus, O., von Haeseler, A., et al. (2014) The evolution of the ribosome biogenesis pathway from a yeast perspective. *Nucleic Acids Res.* 42: 1509–1523.

Fairman-Williams, M.E., Guenther, U.P. and Jankowsky, E. (2010) SF1 and SF2 helicases: family matters. *Curr. Opin. Struct. Biol.* 20: 313–324.

Gabashvili, I.S., Gregory, S.T., Valle, M., Grassucci, R., Worbs, M., Wahl, M.C., et al. (2001) The polypeptide tunnel system in the ribosome and its gating in erythromycin resistance mutants of L4 and L22. *Mol. Cell* 8: 181–188.

Ge, S.J., Yao, X.L., Yang, Z.X. and Zhu, Z.P. (1998) An Arabidopsis embryonic lethal mutant with reduced expression of alanyl-tRNA synthetase gene. *Cell Res.* 8: 119–134.

Gong, Z., Dong, C.H., Lee, H., Zhu, J., Xiong, L., Gong, D., et al. (2005) A DEAD box RNA helicase is essential for mRNA export and important for development and stress responses in Arabidopsis. *Plant Cell* 17: 256–267.

Gong, Z., Lee, H., Xiong, L., Jagendorf, A., Stevenson, B. and Zhu, J.K. (2002) RNA helicase-like protein as an early regulator of transcription factors for plant chilling and freezing tolerance. *Proc. Natl. Acad. Sci. USA* 99: 11507–11512.

Griffith, M.E., Mayer, U., Capron, A., Ngo, Q.A., Surendrarao, A., McClinton, R., et al. (2007) The TORMOZ gene encodes a nucleolar protein required for regulated division planes and embryo development in Arabidopsis. *Plant Cell* 19: 2246–2263.

Guan, Q., Wu, J., Zhang, Y., Jiang, C., Liu, R., Chai, C., et al. (2013) A DEAD box RNA helicase is critical for pre-mRNA splicing, cold-responsive gene regulation, and cold tolerance in Arabidopsis. *Plant Cell* 25: 342–356.

Hang, R., Liu, C., Ahmad, A., Zhang, Y., Lu, F. and Cao, X. (2014) Arabidopsis protein arginine methyltransferase 3 is required for ribosome biogenesis by affecting precursor ribosomal RNA processing. *Proc. Natl. Acad. Sci. USA* 111: 16190–16195.

Hobbie, S.N., Kalapala, S.K., Akshay, S., Bruell, C., Schmidt, S., Dabow, S., et al. (2007) Engineering the rRNA decoding site of eukaryotic cytosolic ribosomes in bacteria. *Nucleic Acids Res.* 35: 6086–6093.

Horiguchi, G., Van Lijsebettens, M., Candela, H., Micol, J.L. and Tsukaya, H. (2012) Ribosomes and translation in plant developmental control. *Plant Sci.* 191–192: 24–34.

Hsu, Y.F., Chen, Y.C., Hsiao, Y.C., Wang, B.J., Lin, S.Y., Cheng, W.H., et al. (2014) AtRH57, a DEAD-box RNA helicase, is involved in feedback inhibition of glucose-mediated abscisic acid accumulation during seedling development and additively affects pre-ribosomal RNA processing with high glucose. *Plant J.* 77: 119–135.

Hua, F.M. and Bedwell, D.M. (2008) Eukaryotic ribosomal RNA determinants of aminoglycoside resistance and their role in translational fidelity. *RNA* 14: 148–157.

Huang, C.K., Huang, L.F., Huang, J.J., Wu, S.J., Yeh, C.H. and Lu, C.A. (2010a) A DEAD-box protein, AtRH36, is essential for female gametophyte development and is involved in rRNA biogenesis in Arabidopsis. *Plant Cell Physiol.* 51: 694–706.

Huang, C.K., Yu, S.M. and Lu, C.A. (2010b) A rice DEAD-box protein, OsRH36, can complement an Arabidopsis atrh36 mutant, but cannot functionally replace its yeast homolog Dbp8p. *Plant Mol. Biol.* 74: 119–128.

Huang, T., Kerstetter, R.A. and Irish, V.F. (2014) APUM23, a PUF family protein, functions in leaf development and organ polarity in Arabidopsis. *J. Exp. Bot.* 65: 1181–1191.

Huang, T.S., Wei, T., Laliberte, J.F. and Wang, A. (2010) A host RNA helicase-like protein, AtRH8, interacts with the potyviral genome-linked protein, VPg, associates with the virus accumulation complex, and is essential for infection. *Plant Physiol.* 152: 255–266.

Hubstenberger, A., Noble, S.L., Cameron, C. and Evans, T.C. (2013) Translation repressors, an RNA helicase, and developmental cues control RNP phase transitions during early development. *Dev. Cell* 27: 161–173.

Ito, T., Kim, G.T. and Shinozaki, K. (2000) Disruption of an Arabidopsis cytoplasmic ribosomal protein S13-homologous gene by transposon-mediated mutagenesis causes aberrant growth and development. *Plant J.* 22: 257–264.

Jarmoskaite, I. and Russell, R. (2011) DEAD-box proteins as RNA helicases and chaperones. *Wiley Interdiscip. Rev. RNA* 2: 135–152.

Jarmoskaite, I. and Russell, R. (2014) RNA helicase proteins as chaperones and remodelers. *Annu. Rev. Biochem.* 83: 697–725.
Jefferson, R.A., Kavanagh, T.A. and Bevan, M.W. (1987) GUS fusions: β-glucuronidase as a sensitive and versatile gene fusion marker in higher plants. *EMBO J.* 6: 3901–3907.
Kant, P., Kant, S., Gordon, M., Shaked, R. and Barak, S. (2007) STRESS RESPONSE SUPPRESSOR1 and STRESS RESPONSE SUPPRESSOR2, two DEAD-box RNA helicases that attenuate Arabidopsis responses to multiple abiotic stresses. *Plant Physiol.* 145: 814–830.
Kaul, M., Barbieri, C.M. and Pilch, D.S. (2005) Defining the basis for the specificity of aminoglycoside–rRNA recognition: a comparative study of drug binding to the A sites of *Escherichia coli* and human rRNA. *J. Mol. Biol.* 346: 119–134.
Khan, A., Garbelli, A., Grossi, S., Florentin, A., Batelli, G., Acuna, T., et al. (2014) The Arabidopsis STRESS RESPONSE SUPPRESSOR DEAD-box RNA helicases are nucleolar- and chromocenter-localized proteins that undergo stress-mediated relocalization and are involved in epigenetic gene silencing. *Plant J.* 79: 28–43.
Kim, J.S., Kim, K.A., Oh, T.R., Park, C.M. and Kang, H. (2008) Functional characterization of DEAD-box RNA helicases in *Arabidopsis thaliana* under abiotic stress conditions. *Plant Cell Physiol.* 49: 1563–1571.
Kim, M.H., Sonoda, Y., Sasaki, K., Kaminaka, H. and Imai, R. (2013) Interactome analysis reveals versatile functions of Arabidopsis COLD SHOCK DOMAIN PROTEIN 3 in RNA processing within the nucleus and cytoplasm. *Cell Stress Chaperones* 18: 517–525.
Kressler, D., Linder, P. and de La Cruz, J. (1999) Protein trans-acting factors involved in ribosome biogenesis in *Saccharomyces cerevisiae*. *Mol. Cell Biol.* 19: 7897–7912.
Kuhn, E. (2012) Toward understanding life under subzero conditions: the significance of exploring psychrophilic 'cold-shock' proteins. *Astrobiology* 12: 1078–1086.
Lafontaine, D., Vandenhaute, J. and Tollervey, D. (1995) The 18S rRNA dimethylase Dim1p is required for pre-ribosomal RNA processing in yeast. *Genes Dev.* 9: 2470–2481.
Lange, H., Sement, F.M. and Gagliardi, D. (2011) MTR4, a putative RNA helicase and exosome co-factor, is required for proper rRNA biogenesis and development in *Arabidopsis thaliana*. *Plant J.* 68: 51–63.
Linder, P. (2006) Dead-box proteins: a family affair—active and passive players in RNP-remodeling. *Nucleic Acids Res.* 34: 4168–4180.
Linder, P. and Fuller-Pace, F.V. (2013) Looking back on the birth of DEAD-box RNA helicases. *Biochim. Biophys. Acta* 1829: 750–755.
Liu, M., Shi, D.Q., Yuan L., Liu, J. and Yang, W.C. (2010) SLOW WALKER3, encoding a putative DEAD-box RNA helicase, is essential for female gametogenesis in Arabidopsis. *J. Integr. Plant Biol.* 52: 817–828.
Lorkovic, Z.J., Herrmann, R.G. and Oelmuller, R. (1997) PRH75, a new nucleus-localized member of the DEAD-box protein family from higher plants. *Mol. Cell Biol.* 17: 2257–2265.
Martin, R., Straub, A.U., Doebele, C. and Bohnsack, M.T. (2013) DExD/H-box RNA helicases in ribosome biogenesis. *RNA Biol.* 10: 4–18.
Medina, J., Catala, R. and Salinas, J. (2011) The CBFs: three arabidopsis transcription factors to cold acclimate. *Plant Sci.* 180: 3–11.
Mingam. A., Toffano-Nioche, C., Brunaud, V., Boudet, N., Kreis, M. and Lecharny, A. (2004) DEAD-box RNA helicases in *Arabidopsis thaliana*: establishing a link between quantitative expression, gene structure and evolution of a family of genes. *Plant Biotechnol. J.* 2: 401–415.
Missbach, S., Weis, B.L., Martin, R., Simm, S., Bohnsack, M.T. and Schleiff, E. (2013) 40S ribosome biogenesis co-factors are essential for gametophyte and embryo development. *PLoS One* 8: e54084.
Nayak, N.R., Putnam, A.A., Addepalli, B., Lowenson, J.D., Chen, T., Jankowsky, E., et al. (2013) An Arabidopsis ATP-dependent, DEAD-box RNA helicase loses activity upon IsoAsp formation but is restored by PROTEIN ISOASPARTYL METHYLTRANSFERASE. *Plant Cell* 25: 2573–2586.
Nazar, R.N. (2004) Ribosomal RNA processing and ribosome biogenesis in eukaryotes. *IUBM Life* 56: 457–465.
Nishimura, K., Ashida, H., Ogawa, T. and Yokota, A. (2010) A DEAD box protein is required for formation of a hidden break in Arabidopsis chloroplast 23S rRNA. *Plant J.* 63: 766–777.
Nishimura, T., Wada, T., Yamamoto, K.T. and Okada, K. (2005) The Arabidopsis STV1 protein, responsible for translation reinitiation, is required for auxin-mediated gynoecium patterning. *Plant Cell* 17: 2940–2953.
O'Connor, M., Gregory, S.T. and Dahlberg, A.E. (2004) Multiple defects in translation associated with altered ribosomal protein L4. *Nucleic Acids Res.* 32: 5750–5756.
Okanami, M., Meshi, T. and Iwabuchi, M. (1998) Characterization of a DEAD box ATPase/RNA helicase protein of *Arabidopsis thaliana*. *Nucleic Acids Res.* 26: 2638–2643.
Owttrim, G.W. (2006) RNA helicases and abiotic stress. *Nucleic Acids Res.* 34: 3220–3230.
Owttrim, G.W. (2013) RNA helicases: diverse roles in prokaryotic response to abiotic stress. *RNA Biol.* 10: 96–110.
Perrot-Rechenmann, C. (2010) Cellular responses to auxin: division versus expansion. *Cold Spring Harb. Perspect Biol.* 2: a001446.
Petricka, J.J. and Nelson, T.M. (2007) Arabidopsis nucleolin affects plant development and patterning. *Plant Physiol.* 144: 173–186.
Phipps, K.R., Charette, J. and Baserga, S.J. (2011) The small subunit processome in ribosome biogenesis—progress and prospects. *Wiley Interdiscip Rev. RNA* 2: 1–21.
Rocak, S., Emery, B., Tanner, N.K. and Linder, P. (2005) Characterization of the ATPase and unwinding activities of the yeast DEAD-box protein Has1p and the analysis of the roles of the conserved motifs. *Nucleic Acids Res.* 33: 999–1009.
Rocak, S. and Linder, P. (2004) DEAD-box proteins: the driving forces behind RNA metabolism. *Nat. Rev. Mol. Cell Biol.* 5: 232–241.
Rodriguez-Galan, O., Garcia-Gomez, J.J. and de la Cruz, J. (2013) Yeast and human RNA helicases involved in ribosome biogenesis: current status and perspectives. *Biochim. Biophys. Acta* 1829: 775–790.
Rosado, A., Li, R., van de Ven, W., Hsu, E. and Raikhel, N.V. (2012) Arabidopsis ribosomal proteins control developmental programs through translational regulation of auxin response factors. *Proc. Natl. Acad. Sci. USA* 109: 19537–19544.
Rosado, A. and Raikhel, N.V. (2010) Application of the gene dosage balance hypothesis to auxin-related ribosomal mutants in Arabidopsis. *Plant Signal Behav.* 5: 450–452.
Rosado, A., Sohn, E.J., Drakakaki, G., Pan, S., Swidergal, A., Xiong, Y., et al. (2010) Auxin-mediated ribosomal biogenesis regulates vacuolar trafficking in Arabidopsis. *Plant Cell* 22: 143–158.
Russell, R., Jarmoskaite, I. and Lambowitz, A.M. (2013) Toward a molecular understanding of RNA remodeling by DEAD-box proteins. *RNA Biol.* 10: 44–55.
Sloan, K.E., Mattijssen, S., Lebaron, S., Tollervey, D., Pruijn, G.J. and Watkins, N.J. (2013) Both endonucleolytic and exonucleolytic cleavage mediate ITS1 removal during human ribosomal RNA processing. *J. Cell Biol.* 200: 577–588.
Stelzl, U. and Nierhaus, K.H. (2001) A short fragment of 23S rRNA containing the binding sites for two ribosomal proteins, L24 and L4, is a key element for rRNA folding during early assembly. *RNA* 7: 598–609.
Stonebloom, S., Burch-Smith, T., Kim, I., Meinke, D., Mindrinos, M. and Zambryski, P. (2009) Loss of the plant DEAD-box protein ISE1 leads to defective mitochondria and increased cell-to-cell transport via plasmodesmata. *Proc. Natl. Acad. Sci. USA* 106: 17229–17234.
Szakonyi, D. and Byrne, M.E. (2011) Ribosomal protein L27a is required for growth and patterning in *Arabidopsis thaliana*. *Plant J.* 65: 269–281.
Thomson, E., Ferreira-Cerca, S. and Hurt, E. (2013) Eukaryotic ribosome biogenesis at a glance. *J. Cell Sci.* 126: 4815–4821.
Vashisht, A.A. and Tuteja, N. (2006) Stress responsive DEAD-box helicases: a new pathway to engineer plant stress tolerance. *J. Photochem. Photobiol. B* 84: 150–160.

Weis, B.L., Palm, D., Missbach, S., Bohnsack, M.T. and Schleiff, E. (2015) atBRX1-1 and atBRX1-2 are involved in an alternative rRNA processing pathway in Arabidopsis thaliana. *RNA* 21: 415–25.

Wieckowski, Y. and Schiefelbein, J. (2012) Nuclear ribosome biogenesis mediated by the DIM1A rRNA dimethylase is required for organized root growth and epidermal patterning in Arabidopsis. *Plant Cell* 24: 2839–2856.

Woolford, J.L., Jr. and Baserga, S.J. (2013) Ribosome biogenesis in the yeast *Saccharomyces cerevisiae*. *Genetics* 195: 643–681.

Xu, R.R., Qi, S.D., Lu, L.T., Chen, C.T., Wu, C.A. and Zheng, C.C. (2011) A DExD/H box RNA helicase is important for K+ deprivation responses and tolerance in *Arabidopsis thaliana*. *FEBS J.* 278: 2296–2306.

Yang, H., Henning, D. and Valdez, B.C. (2005) Functional interaction between RNA helicase II/Gu(alpha) and ribosomal protein L4. *FEBS J.* 272: 3788–3802.

Yao, Y., Ling, Q., Wang, H. and Huang, H. (2008) Ribosomal proteins promote leaf adaxial identity. *Development* 135: 1325–1334.

Zakrzewska-Placzek, M., Souret, F.F., Sobczyk, G.J., Green, P.J. and Kufel, J. (2010) *Arabidopsis thaliana* XRN2 is required for primary cleavage in the pre-ribosomal RNA. *Nucleic Acids Res.* 38: 4487–4502.

Zhou, M.Q., Shen, C., Wu, L.H., Tang, K.X. and Lin, J. (2011) CBF-dependent signaling pathway: a key responder to low temperature stress in plants. *Crit. Rev. Biotechnol.* 31: 186–192.